MATERIALE PLASTICE
https://revmaterialeplastice.ro
https://doi.org/10.37358/Mat.Plast.1964

A Study on the Optimization of Filling Balance for Selective Flexible Flow Path in Family Mold

JAE-WOONG YUN, SANG-SUN LEE, CHUN-KYU LEE*
Kongju National University, Department of Metalmold Design Engineering, 1223-24, Cheonan-daero, Seobuk-gu, Cheonan-si, Chungcheongnam-do, Republic of Korea

Abstract: *In this study, a selective flexible flow path system was developed so that two types (4 cavities) of different shapes, sizes, and weights could be produced simultaneously or individually according for a production plan.The selective flexible flow path system is a method of exchanging sprue parts manufactured in a branched or one-way direction. This method reduces mold costs and provides production flexibility because only the desired cavities can be filled with resin in a multi-cavity mold. Since parts with different shapes and weights are produced simultaneously or separately, it is most important to maintain a uniform filling balance between each cavity. To optimize of filling balance, the optimum value of control factors was derived using the Taguchi technique (DOE) to improve the filling balance. In addition, molds were manufactured under the optimal conditions after checking the filling balance through a CAE analysis. As a result, the flow balance ratio of each product was confirmed to be within 0.6%, and the precision of the product was guaranteed to be within 1%. In this study, it was confirmed once again that the improvement of the filling balance of the family mold had a great influence on the production.*

Keywords*: multi cavity mold, family mold, filling balance, flow path system*

1. Introduction

Injection molds are classified into single cavities and multiple cavities depending on how they are produced. Single cavity method refers to the production of one product in a mold. Many cavities are divided into multi-cavity molds that produce multiple products of the same kind in one mold and family molds that produce products of different shapes in one mold [1, 2]. Recently, many cavity methods have been adopted and produced to improve product productivity and secure competitiveness through cost reduction [3, 4].

The Molding using the family mold causes an imbalance in flow depending on the difference in the flow distance or weight of the resin in the product. This results in product defect due to different injection pressure differences in each cavity. Research continues on the filling imbalance of these multiple cavities. Academic research on filling imbalances, in particular, has been conducted systematically since late 1990 [5-15].

John et al. conducted a study to obtain a uniform distribution of shear rates in the secondary runner by changing the direction of flow to a part called the Melt Flipper TM [16]. Han et al. compared the amorphous resin and crystalline resin with respect to the flow path charge imbalance phenomenon generated in a plurality of cavity hot runner molds [17]. Park et al. developed and applied a variable runner system to solve the filling imbalance between products, confirming that the flow balance effect can be obtained [18]. Park et al. adjusted the valve diameter of the hot runner mold and improved the flow balance using the time difference of the Sequence Valve [19]. And Park et al. were studied to make a filling balance of multiple cavities by uniformly melting temperature through screw rotation [20]. Jeong et al. presented a new system using the Runner Core Pin in the runner to address the imbalance in filling of the geometrically balanced runners in multiple cavity molding schemes [21].

**email: ckt1230@kongju.ac.kr*

Kang et al. changed the filling imbalance phenomenon of multiple cavities to form conditions for two resins with different resin characteristics, thus grasping the temperature distribution and cavity imbalance relationship of runners [22]. Kazmer et al. describe the capability of the multi-cavity pressure control system and the function of improving the quality of the molded parts. Results show that this technology enables significant process flexibility to randomly balance flows, move knit lines, and control multiple part dimensions [23]. Orzechowski et al. described a low-cost process monitoring and control system using nozzle-based pressure and temperature sensors. Furthermore, full-scale industrial, experimental results are presented, showing that temperature and pressure measurements of injector nozzles can effectively control melt quality and shot size uniformity [24]. Wilczyński et al. used three optimization techniques to study and optimize the charging imbalance of geometrically balanced injection molds. It is a response surface methodology (RSM), the Taguchi method, and an artificial neural network (ANN) [9]. Cook et al. presented experimental data on multi-cavity moldings that show significant flow imbalances despite geometrically balanced supply systems. As a result, we can see the dependence of imbalance on the relative size of cooling and shear heating on the mold wall [25]. Huang et al. aim to improve the flow balance by modifying the runner system design. The experimental results indicate that the tapering H-type runner system can improve flow balance [26].

To date, research trends have conducted studies on the basic experiments of imbalances according to the type of molding condition or resin to theoretically identify the imbalance in charge of runners in many cavities with geometric balance. In addition, molds were designed structurally to address filling imbalance. And in family molds using hot runner system, the time difference and diameter of the gate valve were adjusted to improve the quality of the product. However, research on a runner system for a family mold that can produce parts with different shapes and weights simultaneously or individually according to the production plan has not been conducted.

In this study, a selective flexible flow path system was developed so that two types (4 cavities) of different shapes, sizes, and weights could be produced simultaneously or individually. The optimal condition of filling balance was analyzed using the Taguchi technique (DOE) to uniformly charge 2 types of products with different shapes, sizes and weights to derive the optimal solution. In addition, the filling balance was verified and molded through the CAE molding analysis under the optimal conditions derived. The flow balance of the flow path system was verified through the test injection. In addition, the temperature distribution of the manifold and gate nozzle affecting the flow balance was uniformly constructed and verified through thermal balance analysis to minimize the impact of the product's flow balance.

2. Materials and methods

2.1. Selective flexible flow path system

In Figure 1, a selective flexible flow path system was developed using two models of refrigerator guide rail parts as test subjects. The selective flexible flow path system is a system that can produce parts simultaneously (A+B) or individually (A, B) according to the production plan. The selective flexible flow path system can produce parts simultaneously or individually with one mold by exchanging the sprue part that can fill the resin coming from the injection machine in a branched or unidirectional direction. Since parts with different shapes and weights are produced simultaneously or separately, it is most important to maintain a uniform filling balance between each cavity.

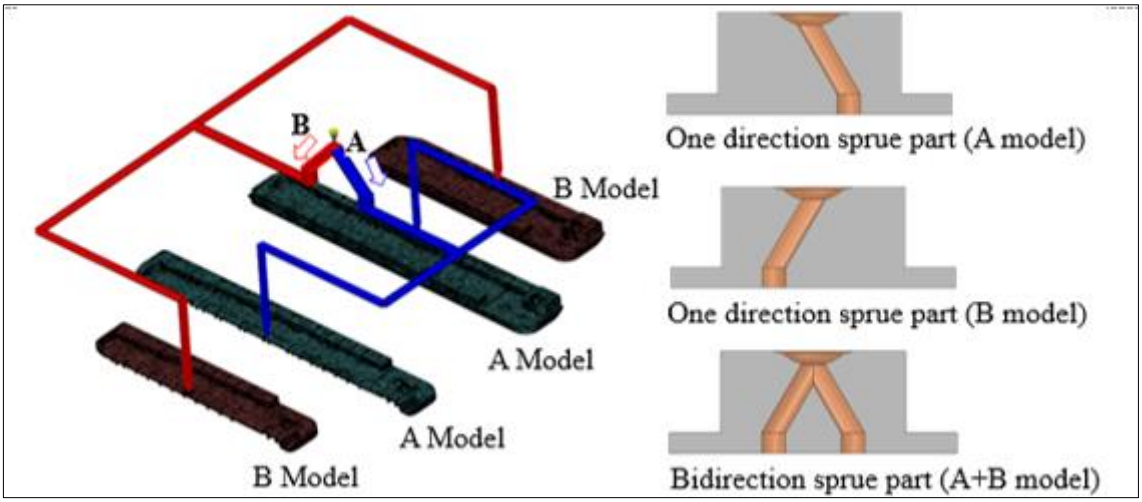

Figure 1. Selective flexible flow path system

2.2. Definition of experimental model

The experimental model in Figure 2 is a guide rail for refrigerators (A/Left, A/Right, B/Left, B/Right) with different shapes and 1.3 times the weight difference. Table 1 shows the characteristic dimensions of the rail A/B model.

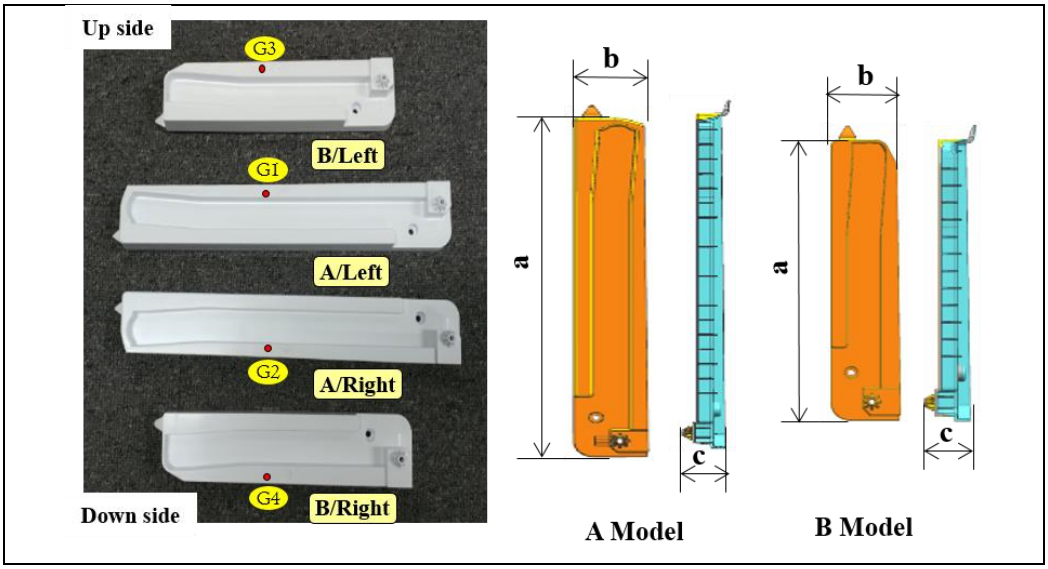

Figure 2. Specification and shape of experimental model

Table 1. Dimensions and weight of experimental model

Model	Dimensions & weight				
	a (mm)	b (mm)	c (mm)	Weight(g)	Average of thickness(mm)
A	344.5	43	37.1	90.6	2.5
B	247.7	53.3	36.9	67.3	2.5

2.3. Definition of the control factors influencing on the filling balance

Factors affecting uniform filling up to the end of each product of the family mold with hot runner system include the arrangement of runners to each cavity, nozzle specification, flow path length, flow path diameter, gate diameter, injection molding conditions (mold temperature, resin temperature, injection velocity, injection pressure, injection time, etc), temperature control of the manifold, manufacturing precision of mold and flow characteristics of the resin. However, in order to determine

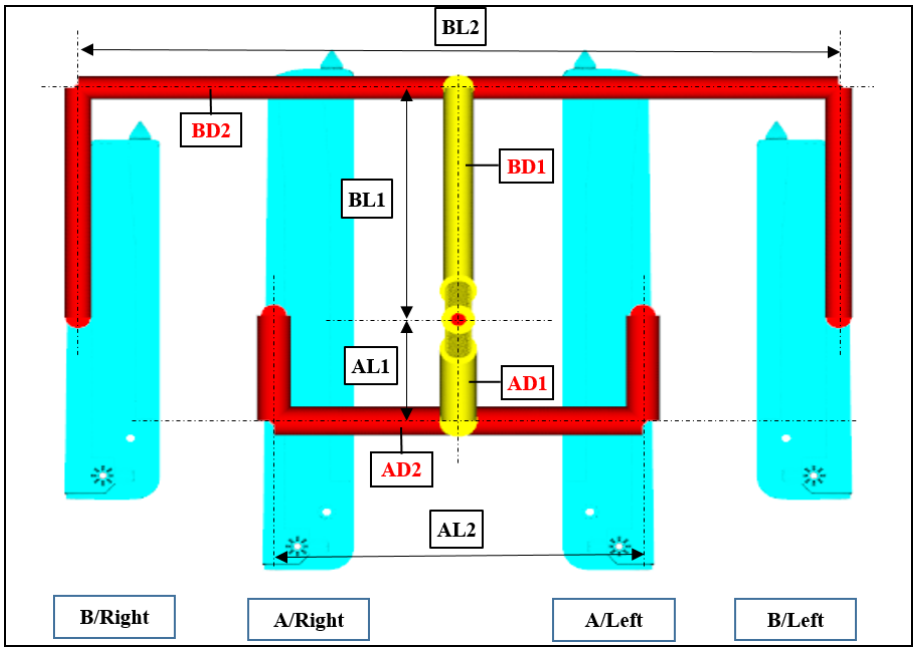

Figure 3. Product layout of the molding analysis models

the location of each product with different shapes and weights in a mold, the length and diameter of the runner must first be selected. In this experiment, for the filling balance of each cavity, the control factor was chosen as the runner diameter and length of the manifold.

Figure 3 is the layout of this experimental variables as control factor. The length and diameter of the Spruce to the Primary Runner Branch of Model A's Hot Runner System are marked AL1, AD1. The length and diameter of the second runner branch from the primary runner branch to the gate entrance are marked AL2, AD2. Model B also selected BL1, BL2, BD1 and BD2 with the same flow lengths and diameters as model A.

2.4. Calculation of flow balance ration difference with CAE analysis

Based on the Taguchi technique [27-30], this experiment was performed with a orthogonal array mixing level design $L^{18}(2^1 \times 3^7)$. Table 2 describes the eight control factors applied in the experiment as Mark A~H. And factor A defined 2 levels (Φ12, 15) and factor B to H each defined 3 levels. The size and range of the number of levels was chosen based on the size constraints of the mold because of specifications of the injection molding machine, the specifications of the Manifold manufacturer and the experience of a professional designer.

Table 2. Level and control factors

No.	Control factors	Mark	Level		
			1	2	3
1	A Model Diameter (AD1)	A	12	15	
2	A Model Diameter (AD2)	B	8	10	12
3	A Model Length (AL1)	C	90	115	135
4	A Model Length (AL2)	D	107	117	127
5	B Model Diameter (BD1)	E	8	10	12
6	B Model Diameter (BD2)	F	6	8	10
7	B Model Length (BL1)	G	145	150	155
8	B Model Length (BL2)	H	222	232	242

Table 3 shows the results of $L^{18}(2^1 \times 3^7)$ orthogonal arrangement. The inner arrangement was marked with eight control factors (Runner's diameter and length, A-H) and the number of levels (1, 2, 3). In addition, the noise coefficient for the outer array side was chosen as the injection nozzle temperature in three cases 220, 230 and 240℃. And 18 CAE mold analyses were performed for each selected nozzle temperature, and the weight of the A and B cavities at 90% of the total mass was measured to calculate the flow balance and to show the difference.

For example, the flow-balancing rate can be calculated as in Figure 4. When Model A and B are simultaneously filled with 88.2% of the total filling weight, the estimated charge weight is 88.2g for A and 61.7g for B. Through CAE analysis, the actual charge weight of A and B is calculated as 90g and 60g. If the flow balance of each product is calculated using equation (2-1), A is calculated 102% and B is 97.2%. That means product A was overcharged by 2 %, while product B was uncharged by 2.8 %. Thus, the final difference in the flow-balance ratio of A and B products can be represented at 4.8%.

$$Flow\ balance\ ratio[\%] = \frac{Actual\ charge\ for\ each\ cavity[g]}{Estimated\ charge\ for\ each\ cavity[g]} \times 100 \quad (2\text{-}1)$$

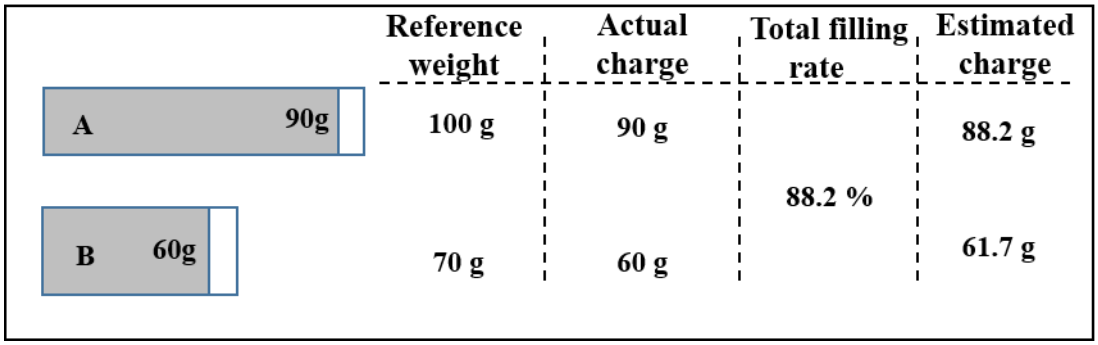

Figure 4. Example of calculating the flow balance ratio

Table 3. Orthogonal arrays and flow balance ratio difference ($L^{18}(2^1 \times 3^7)$)

No.	Control factors and levels								Flow balance ratio difference		
	A	B	C	D	E	F	G	H	220℃	230℃	240℃
1	1	1	1	1	1	1	1	1	37.63	29.36	37.72
2	1	1	2	2	2	2	2	2	28.19	21.17	32.13
3	1	1	3	3	3	3	3	3	18.51	16.21	20.43
4	1	2	1	1	2	2	3	3	30.73	27.34	32.60
5	1	2	2	2	3	3	1	1	4.80	1.60	2.68
6	1	2	3	3	1	1	2	2	10.63	6.58	7.47
7	1	3	1	2	1	3	2	3	30.08	26.55	33.30
8	1	3	2	3	2	1	3	1	39.60	30.83	39.94
9	1	3	3	1	3	2	1	2	35.92	26.54	38.75
10	2	1	1	3	3	2	2	1	33.60	24.02	37.69
11	2	1	2	1	1	3	3	2	14.85	11.12	18.46
12	2	1	3	2	2	1	1	3	38.50	30.79	39.52
13	2	2	1	2	3	1	3	2	39.10	30.64	39.47
14	2	2	2	3	1	2	1	3	34.82	28.29	35.41
15	2	2	3	1	2	3	2	1	20.39	15.22	22.82
16	2	3	1	3	2	3	1	2	30.17	25.51	33.23
17	2	3	2	1	3	1	2	3	40.69	31.67	41.07
18	2	3	3	2	1	2	3	1	35.95	29.56	37.28

2.5. Deriving the optimal value of control factors

The S/N ratio of the analysis results using the statistical analysis program MINITAB according to the prepared orthogonal array table is shown in Table 4. If you look at the degree of influence rank that each control factor (A-H) has on the optimal condition, the most influential factors are the control factor B (diameter) of model A, the factor F (diameter) of the model B, the factor C (length) of the model A, the factor A (diameter) of the model A, the factor H (length) of the model B, the factor E (diameter) of the model B, the factor D (length) of the model A, and the least influential factor was G (length) of the model B. The contribution rate (Rho) of the control factor is about 63.8% of the total variation in the diameter (A, B, E, F) of the runner. This is judged to have a higher diameter than the runner's length in the manifolder.

Figure 5 shows the main effects of S/N (signal-to-noise factor) ratio due to the difference in the flow rate of charge as the locale characteristic. In Figure 5, the value in red dotted line represented the optimal level value and the level value of the optimal factor was derived, such as Table 5. The optimal level values are: diameters from sprue to bifurcation (AD1, A): Ø 12 mm in model A, diameter from bifurcation to product (AD2, B): Ø 10 mm, distance from sprue to bifurcation (AL1, C): 115mm in model A, distance from bifurcation to product (AL2, D): 117mm in model B, diameter from sprue to bifurcation (BD1, E): Ø 12 mm, diameter from bifurcation to product (BD2, F): Ø 10 mm, distance from bifurcation to bifurcation (AL1, G): 145mm, and distance from bifurcation to product (AL2, H): 222mm. The optimal result was derived and the molding analysis was conducted.

Table 4. Analysis of significance of S/N ratio of factors

Level	A	B	C	D	E	F	G	H
1	-26.13	-28.34	-30.18	-28.72	-27.28	-29.15	-27.18	-26.58
2	-29.38	-24.34	-26.02	-27.00	-29.41	-30.06	-27.43	-27.05
3		-30.57	-27.06	-27.54	-26.57	-24.04	-28.65	-29.62
Delta	3.25	6.23	4.16	1.72	2.83	6.02	1.48	3.04
Rank	4	1	3	7	6	2	8	5
Rho (%)	11.31	21.68	14.48	5.99	9.85	20.95	5.15	10.58

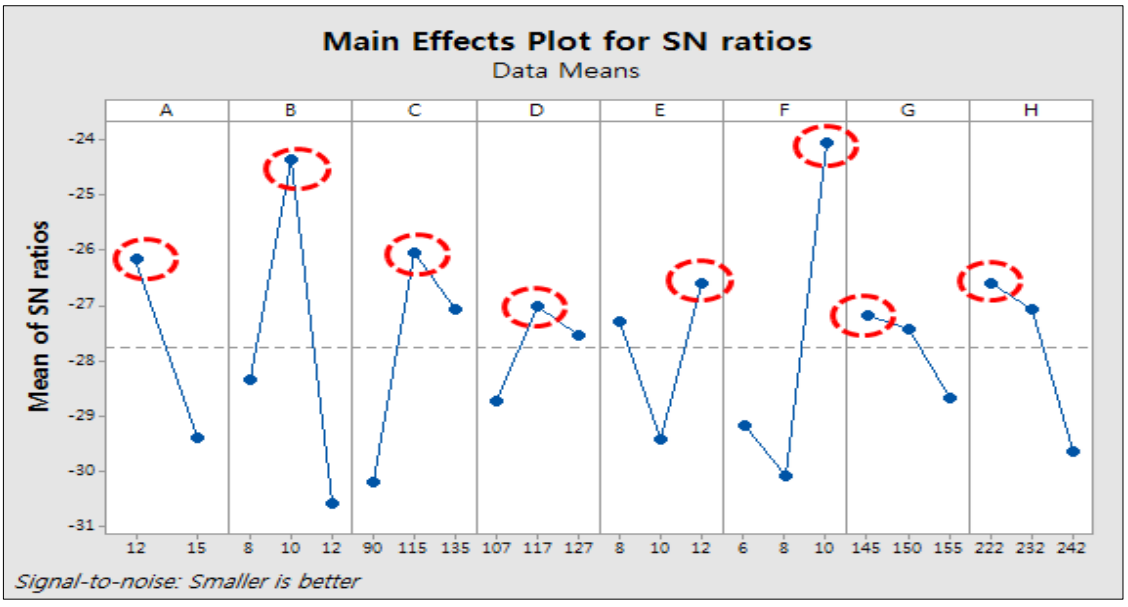

Figure 5. Main effects plot for S/N ratios

Table 5. Optimal factors of S/N ratio

No.	Control factors							
	AD1	AD2	AL1	AL2	BD1	BD2	BL1	BL2
Optimal factor	12	10	115	117	12	10	145	222

2.6. CAE analysis verification with optimized control factors

The analysis software used Moldflow version 2019 and the mesh type was applied as a dual domain. The aspect ratio of mesh for analysis is set to 20 and the number of mesh is set to 104,582. The resin used in the molding analysis is LG Chem's HIPS HR60 for the high impact. The condition applied to the molding analysis is that the upper mold temperature is set at 40℃ and the lower mold temperature is set at 30℃ because the appearance characteristics are required for the product. The injection time is 1.52s, the nozzle temperature and runner temperature are set at 230℃.

Figure 6 shows the results of the filling analysis for the simultaneous four cavities optimized according to the experimental planning method. The flow balance was seen filling 99% of all four cavities with injection time of 1.52s.

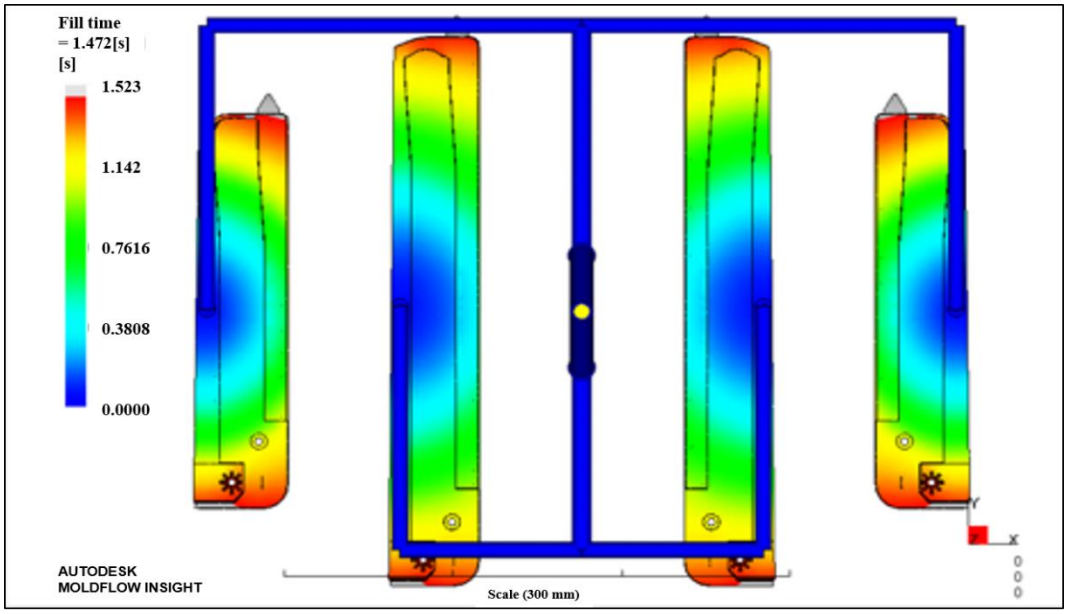

Figure 6. CAE Analysis of 4 cavities injection molding at 1.52s

2.7. Experimental conditions

LS Maron's high-speed, precise electric injection machine WIZ 350E was used in this experiment. Figure 7 shows the family mold on the injection machine. (a) is a movable-side mold; (b) is a fixed-side mold. Since family molds produce multiple products simultaneously in one injection molding, they pose the problem of having to stop production when modifications and repairs occur. To solve this problem of maintenance, molds were made separately for each cavity, and product production was possible while the mold was being repaired. To minimize the effects of flow balancing and increase cooling efficiency on the bottom ribs of the product, moldmax, a highly heat-conducting material, was manufactured in a movable-side mold.

Table 7 shows the molding condition applied to the injection experiment. Based on the CAE analysis results, injection molding conditions were set at 25s, 40℃ for fixed-sided molds, 30℃ for movable molds and 230℃ for resin. Table 8 is the property statement of resin used for the experiment, while resin used LG Chem's HIPS HR60.

(a) Movable side mold (b) Fixed side mold

Figure 7. Family Mold for experiment

Table 7. Injection molding condition of experiment

Index	Unit	Injection molding condition
Cavity plate temp.	℃	40
Core plate temp.		30
Hot runner temp.		230
Barrel Melt temp.		180~230
V/P switch-over	mm	4.22
Injection time	sec	1.4
Holding time	sec	3.5
Holding pressure	MPa	40
Cooling time	s	25

Table 8. Properties of experimental resin

Property	Test method	Units	Value
Tensile strength	ASTM D638	kg/cm^2	290
Flexural strength	ASTM D790	kg/cm^2	460
Rockwell hardness	ASTM D785	HRR	99
Deflection temperature	ASTM D648	℃	93
Flammability	UL94	class	HB
classification			
Melt flow rate	ASTM D1238 (200℃/5kg)	g/10min	5.3
Shrinkage rate	ASTM D955	%	0.4 ~ 0.8
Mold temperature	-	℃	40 ~ 70
Drying time	-	hrs	2 ~ 4
Drying temperature	-	℃	80
Moisture content	-	%	0.01

3. Results and discussions

3.1. Experimental results and analysis for 4 cavity injection molding

In Figure 8, the simultaneous 4 cavity injection molding results were compared with the CAE analysis results. The injection rate was set at 50 percent of the maximum speed of the injection period, and the filling amount was different, with 46, 63, 94, and 101 % of the total charge. The results of the test injection molding and CAE analysis were visually verified and the weight of each cavity was measured to produce the results with a flow-balance ratio. The CAE analyzed balance has been identified as a pattern that is almost identical to the actual injection molding.

Figure 9 and Table 9 are the result of the flow-balance ratio according to the weight of the four cavities. The difference in the flow rate between each cavity shows that the outer B model tends to charge faster than the central A model, but the balance rate gradually becomes similar. This shows that the flow characteristics of the resin vary depending on the shape of the product (Rib and thickness variation). The flow-balance ratio of 101 % of the final charge was 100.3 % for Model B, which is 0.23 g more than the expected weight. The flow-balance ratio of model A stood at 99.7 %, 0.23 g less than expected weight. The balance of the overall flow was found to be less than 0.6 %.

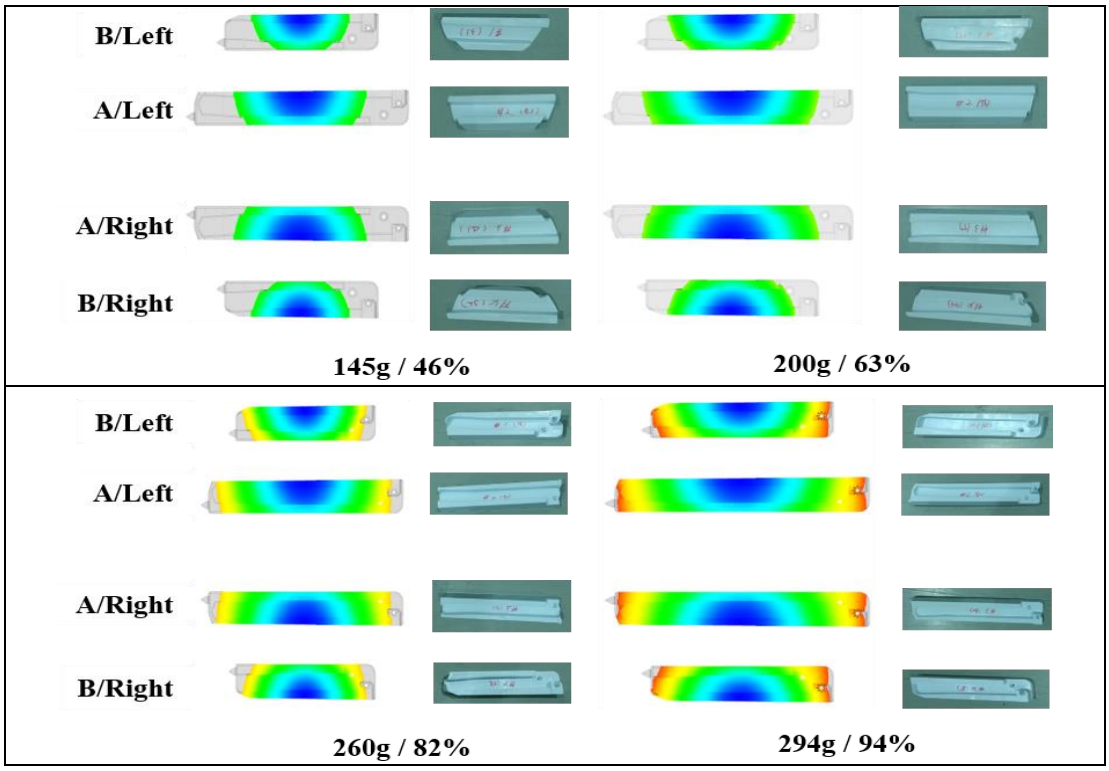

Figure 8. Results comparison of CAE analysis and actual injection molding (A+B model)

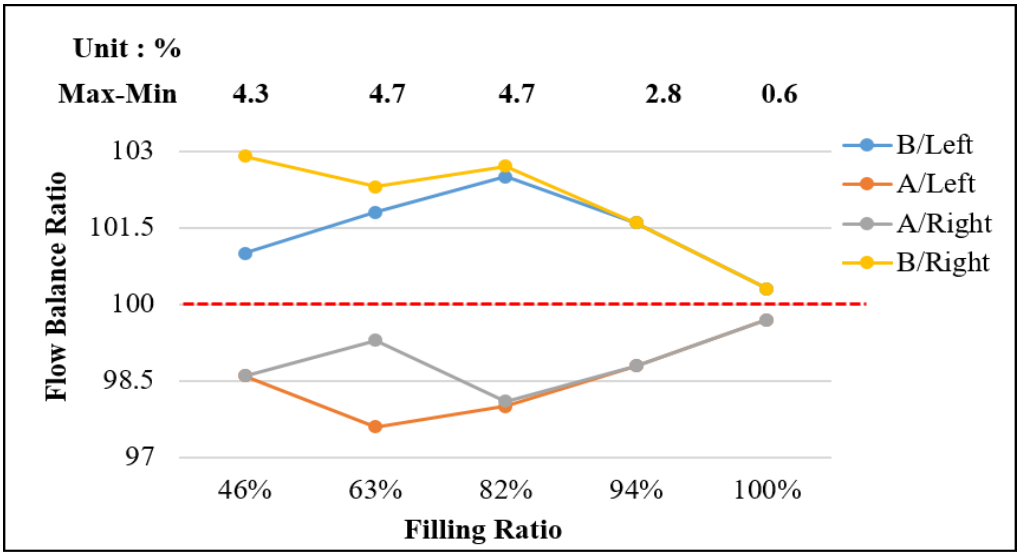

Figure 9. Graph of flow balance ratio on 4 cavity

Table 9. Comparison of flow balance ratio of 4 cavity

Cavity	Reference products		46%		63%		94%		101%	
	W(g)	Balance ratio	W(g)	Balance ratio	W(g)	Balance ratio	W(g)	Balance ratio	W(g)	Balance ratio
B/Left	67.3	100%	31.2	101.0%	43.4	101.8%	64.5	101.6%	68.0	100.3%
A/Left	90.6	100%	41.0	98.6%	56.0	97.6%	83.0	98.8%	91.0	99.7%
A/Right	90.6	100%	41.0	98.6%	57.0	99.3%	83.0	98.8%	91.0	99.7%
B/Right	67.3	100%	31.8	102.9%	43.6	102.3%	64.5	101.6%	68.0	100.3%
Total	315.8	100%	145.0		200.0		295.0		318.0	

Table 10 shows the dimensional results of each product when the charge rate is 100%. The five measured products were samples 24 h after they were produced with the final injection condition. The measurement measured the (a) overall length of the product, (b) overall width, and (c) the overall height of the product. Overall, the dimensions met the reference tolerance criteria, the maximum dimension difference was measured to be 0.08 mm in overall width of the A/Right product and 0.08 mm in overall length of the B/Right product. The minimum dimension difference was measured to be 0.00mm in the overall height of B/Left products. When the flow balance of each cavity is optimized, the dimensional distribution of the product can be confirmed to be stable.

Table 10. Dimensional measurement result of 4 cavities

Cavity	No	Dimen-sions (mm)	Tolerance (mm)	T1-1 (mm)	T1-2 (mm)	T1-3 (mm)	T1-4 (mm)	T1-5 (mm)	Average (mm)	Differ-ence (mm)
B/Left	a	247.70	±0.5	247.64	247.62	247.64	247.64	247.65	247.64	0.06
	b	53.30	±0.3	53.23	53.25	53.26	53.25	53.26	53.25	0.05
	c	36.90	±0.3	36.91	36.89	36.90	36.89	36.90	36.90	0.00
A/Left	a	344.50	±0.5	344.49	344.48	344.49	344.48	344.49	344.49	0.01
	b	43.00	±0.3	42.95	42.96	42.95	42.96	42.95	42.95	0.05
	c	37.10	±0.3	37.04	37.06	37.05	37.06	37.05	37.05	0.05
A/Right	a	344.50	±0.5	344.47	344.45	344.45	344.45	344.45	344.45	0.05
	b	43.00	±0.3	42.91	42.92	42.92	42.92	42.92	42.92	0.08
	c	37.10	±0.3	37.02	37.03	37.04	37.03	37.04	37.03	0.07
B/Right	a	247.70	±0.5	247.60	247.62	247.61	247.63	247.62	247.62	0.08
	b	53.30	±0.3	53.25	53.22	53.27	53.22	53.27	53.25	0.05
	c	36.90	±0.3	36.86	36.82	36.84	36.82	36.84	36.84	0.06

3.2. Experimental results and analysis for 2 cavity injection molding

In Figure 10, the individual 2 cavity injection molding of A model results were compared with the CAE analysis results. The injection rate was set at 50 percent of the maximum speed of the injection period, and the filling amount was different, with 41, 57, 75, and 92 % of the total charge.

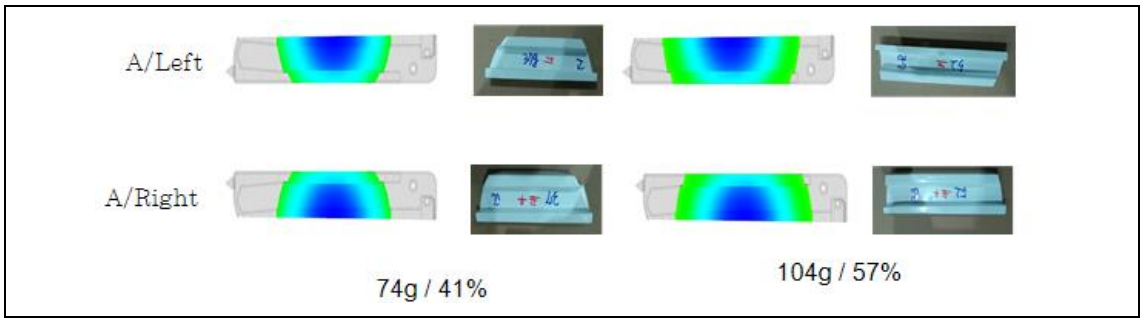

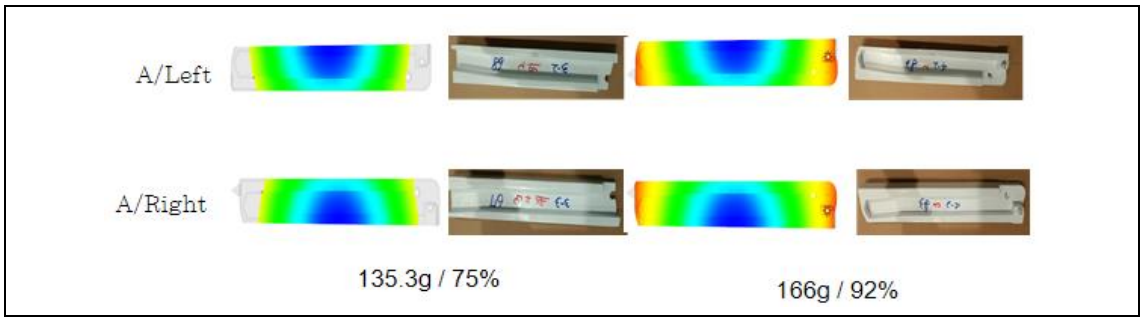

Figure 10. Results comparison of CAE analysis and actual injection molding (A model)

In Figure 11, the individual 2 cavity injection molding of B model results were compared with the CAE analysis results. The injection rate was set at 50 percent of the maximum speed of the injection period, and the filling amount was different, with 46, 74, 88, and 97 % of the total charge. The results of the test injection molding and CAE analysis of A and B model were visually verified and the weight of each cavity was measured to produce the results with a flow-balance ratio. The CAE analyzed balance has been identified as a pattern that is almost identical to the actual injection molding.

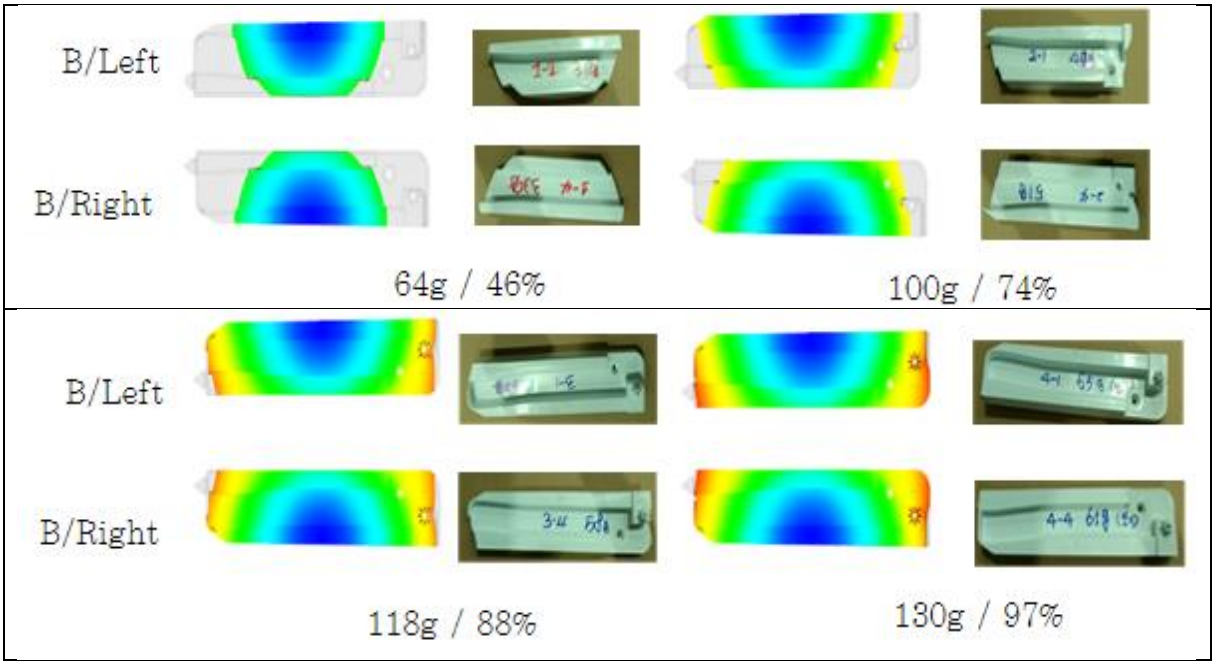

Figure 11. Results comparison of CAE analysis and actual injection molding (B model)

Table 11 shows the results of the flow filling rate versus weight for the individual two-cavity A models. When the filling ratio was 75%, the flow filling ratio between the cavities differed by about 1%. However, as the filling ratio gradually increased, the difference in the flow filling ratio of each cavity converges to 0%, and after 92% filling, the molding balance between the cavities is maintained the same and 100% filling was obtained.

Table 11. Comparison of flow balance ratio of 2 cavity (A Model)

Cavity	Reference products		41%		57%		75%		92%	
	W(g)	Balance ratio	W(g)	Balance ratio	W(g)	Balance ratio	W(g)	Balance ratio	W(g)	Balance ratio
A/Left	90.6	100%	37.0	100.0%	52.0	100.0%	68.0	100.5%	83.0	100.0%
A/Right	90.6	100%	37.0	100.0%	52.0	100.0%	67.3	99.5%	83.0	100.0%
Total	181.2	100%	74.0		104.0		135.3		166.0	

Table 12 shows the results of the flow filling rate versus weight for the individual two-cavity B models. At the beginning of the filling, B/Left progressed slower than B/Right, so there was a difference of about 6.2%, but at 97% of the filling amount, the molding balance of each cavity was the same and 100% filling. This phenomenon can be seen that the flow characteristics change depending on the shape (rib, thickness, etc.) of B model.

Table 12. Comparison of flow balance ratio of 2 cavity (B Model)

Cavity	Reference products		46%		74%		88%		97%	
	W(g)	Balance ratio	W(g)	Balance ratio	W(g)	Balance ratio	W(g)	Balance ratio	W(g)	Balance ratio
B/Left	67.3	100%	31.0	96.9%	49.0	98.0%	60.0	101.7%	65.0	100.0%
B/Right	67.3	100%	33.0	103.1%	51.0	102.0%	58.0	98.3%	65.0	100.0%
Total	134.6	100%	64.0		100.0		118.0		130.0	

For the optimization of control factors, the Taguchi method and S/N ratio of the analysis are already used in various fields. In particular, Wilczyński et al. [9] and Tsai et al. [11] used this method to optimize the filling balance in multi cavity mold through injection molding simulation. In this study, control factors were optimized using this method, and a family mold was manufactured using the optimized diameter and length. To verify the selective flexible flow path system, 4-cavity and 2-cavity injection molding experiments were conducted, and the agreement between the analysis results and the actual product was verified.

4. Conclusions

In this study, a selective flexible flow path system was developed for the refrigerator guide rail parts so that two types (4 cavities) of different shapes, sizes, and weights could be produced simultaneously or individually according for a production plan. The method of exchanging sprue part allows flexible production of desired parts with one mold. Since control factors (length, diameter) of the runner have a great influence on the filling balance, the optimization before mold manufacturing is essential. The results of this study were summarized as follows:

- to optimize the filling balance of family molds, Taguchi technique was found to be a very useful tool and very effective in finding optimal conditions for control factors;

- an analysis of factors affecting uniform filling of the product showed that the diameter of the manifolder runner was more influential than its length. The impact was about 63.8 % in diameter and 36.2 % in length. The largest diameter factor was the diameter (AD2) from the runner branch of Model A to the product;

- the optimal runner and diameter values for this experimental model are the diameter of the A model from the sprue to the junction (AD1):Φ12 mm, the diameter from the bifurcation point to the product (AD2):Φ10 mm, the distance from the spruce to the junction of model A (AL1) :115 mm, the distance from the bifurcation point to the product (AL2):117 mm, the diameter (BD1) of model B from the sprue to the junction (Φ12 mm), the diameter from branch point to product (BD2):Φ10 mm, the distance from the spruce to the bifurcation point (AL1) of model B:145 mm and the distance from the bifurcation point to the product (AL2):222 mm;

- in the case of simultaneous 4 cavity injection molding, the flow rate of charge was found to be 99.7% of Model A and 100.3% of Model B, and the difference in the overall flow balance was within 0.6%. In addition, the difference in dimensions between each product is maximal 0.08mm and the tolerance of error was minimized to 0.3% of the total dimension.

- in the case of individual 2 cavity injection molding, the molding balance of each cavity obtained the same and 100% filling from 92% of the filling amount at A model and 97% of the filling amount at B model.

In the future, the study for the optimization of filling balance of multiple cavities (6 and 8 Cavities) in the area of family mold should be done continuously for increasing the productivity. Thus, research should be activated to quantify the filling balance by deriving a formula for the relationship of the runner diameter and length according to the weight and size difference.

Acknowledgments: This work was supported by the research grant of the Kongju National University in 2019.

References

1.KLAUS, S., Mold-Marking Handbook, *Carl Hanser Verlag Munchen Wien*, 1983, 23-35.
2.MENGES, M., SpritzgiβWerkzeuge, *Carl Hanser Verlag Munchen Wien*, 1991, 136-154.
3.WON, S, T., HEO, Y, M., GO, Y, B., KIM, G, H., YOON, G, S., Trends of Injection Molding Technology, *The Korean Society for Technology of Plasticity*, 23(3), 2014, 184-188.
4.CHAN, I, W, M., MARTYN, P., KWONG, C, K., SZETO, W, H., Automation and optimization of Family Mould Cavity and Runner Layout Design (FMCRLD) using genetic algorithms and mould layout design grammars, *Computer-Aided Design*, 47, 2014, 118~133.
5.M. R. KAMAL, et al., 1987, Dynamics and control of pressure in the injection molding of thermoplastics, Polymer Engineering and Science, Vol. 27, pp. 1403-1410
https://doi.org/10.1002/pen.760271809
6.J. P. COULTER, 2003, Cavity specific control of melt flow during injection molding processes, Conference proceedings of ASME International Mechanical Engineering Congress & Exposition, Washington, D.C., Vol. 3
7.REIFSCHNEIDER, L. G. (2001). Documenting and simulating flow segregation in geometrically balanced runners. Journal of Injection Molding Technology, 5(4), 208.
8.WILCZYÑSKI, K., NAROWSKI, P., Simulation Studies on the Effect of Material Characteristics and Runners Layout Geometry on the Filling Imbalance in Geometrically Balanced Injection Molds, *Polymers*, 2019, 11, 639.
9. WILCZYNSKI, K., NAROWSKI, P., A Strategy for Problem Solving of Filling Imbalance in Geometrically Balanced Injection Molds, *Polymers*, 2020, 12, 805.
10. WILCZYNSKI, K., WILCZYŃSKI, K., NAROWSKI, P., Experimental and simulation studies on filling imbalance in geometrically balanced runner systems of multi-cavity injection molds, *Polimery*, 2015, 60, 411-421.
11.TSAI, H. H., WU, S. J., LIU, J. W., CHEN, S. H., LIN, J. J., Filling-Balance-Oriented Parameters for Multi-Cavity Molds in Polyvinyl Chloride Injection Molding, *Polymers*, 2022, 14, 3483.
12.JEON, K. I., NOH, S. K., KIM, D. H., A study on the runner system for filling balance in mul-ti-cavity injection molds, *Journal of the Korea Academia-Industrial cooperation Society*, 2011, 12(4), 1581-1588.
13. GIM, J. S., TAE, J. S., JEON, J. H., CHOI, J. H., RHEE, B. O., Detection method of filling imbalance in a multi-cavity mold for small lens, *International Journal of Precision Engineering and Manufacturing*, 2015, 16(3), 531-535.
14.SANCHEZ-CASTILLO, L., NEDELCU, D., FRANCISCO-MARQUEZ, M., Redesign of layout runner in rubber injection molding for filling of a multi-cavity mold, *Materiale Plastice*, 2021, 58(3), 121-128.
15.CHEN, J. B., SHEN, C. Y., YOKOI, H., A Study on Influence of Resin Temperature on Filling Balance of Multi-Cavity Molds, *In Advanced Materials Research*, 2010, 87, 550-554)
16.JOHN, P, B., JACK, H, Y., MATTHEW, J, J., Mold filling imbalances in geometrically balanced runner system", Journal of Reinforced Plastics and Composites, 18(6), 1999
17. HAN, S, R., KANG, C, M., HAN, K, T., JEONG, Y, D., A Study on the Filling Imbalances between Multi-Cavity in Hot-Runner Mold, *Journal of the Korean Society of Precision Engineering*, 22(9), 2005, 173-178.

18. PARK, H, P., CHA, B, S., RHEE, B, O., An experimental study for the filling balance of the family mold, *The Korean Society for Technology of Plasticity*, 15(1), 2006, 47-56.
19. PARK, J, H., YOON, K, W., KO, C, O., SEO, S, W., KIM, S, J., Study on Improving Flow Balance and Clamp Force of Family Mold for Refrigerator Shel, *J. Korean Soc. Manuf. Technol. Eng.*, 23(6), 2014, 561-568.
20. PARK, S, R., KIM, J, H., LYU, M, Y., A Novel Runner Design for Flow Balance of Cavities in Multi-Cavity Injection Molding, *Polymer (Korea)*, 33(6), 2009, 561-568.
21. JEONG, Y, D., Development of New Runner System for Filling Balance in Multi Cavity Injection Mold, *Transactions of Materials Processing*, 15(1), 2006, 42-46.
22. KANG, M, A., LYU, M, Y., Investigation of the Filling Unbalance and Dimensional Variations in Multi-Cavity Injection Molded Parts, *Polymer (Korea)*, 32(6), 2008, 501-508.
23.KAZMER, D., BARKAN, P., (1997), The process capability of multi-cavity pressure control for the injection molding process. Polym Eng Sci, 37: 1880-1895. https://doi.org/10.1002/pen.11838
24.ORZECHOWSKI, S., PARIS, A., DOBBIN, C.J., (1998). A process monitoring and control system for injection molding using nozzle-based pressure and temperature sensors. The Journal of injection molding technology, 2, 141-148
25.COOK, P., COSTA, F., KIETZMANN, C., YU, H., (2005, May). Prediction of flow imbalance in geometrically balanced feed systems. In ANTEC-CONFERENCE PROCEEDINGS- (Vol. 2, p. 108).
26.HUANG, T. C., HUANG, P. H., YANG, S. Y., KO, T. Y., Improving flow balance during filling a multi-cavity mold with modified runner systems. Int. Polym. Process. 2008, 23, 363–369. [CrossRef]
27. RANJIT, K, R., Design of Experiments Using the Taguchi Approach, 2001, 369-404.
28. PHADKE, M, S., Quality Engineering Using Robust design, *Prenice-Hall*, 1989.
29. LEE, J, K., YE, S, D., OH, H, O., MIN, B. H., Design for Injection Molding Process of Part Shoes by Design of Experiment, *The Korean Society for Technology of Plasticity*, 2005, 423-426.
30. SHIN, H. Y., PARK, E. S., Analysis of Incomplete Filling Defect for Injection-Molded Air Cleaner Cover Using Moldflow Simulation, *Journal of Polymers*, 2013, 13

Manuscript received: 26.05.2022